Article

Activation of the Sulfhydryl Group by Mo Centers: Kinetics of Reaction of Benzyl Radical with a Binuclear Mo(μ-SH)Mo Complex and with Arene and Alkane Thiols

James A. Franz, Jerome C. Birnbaum, Douglas S. Kolwaite, John C. Linehan, Donald M. Camaioni, and Michel Dupuis

J. Am. Chem. Soc., **2004**, 126 (21), 6680-6691• DOI: 10.1021/ja049321r • Publication Date (Web): 08 May 2004

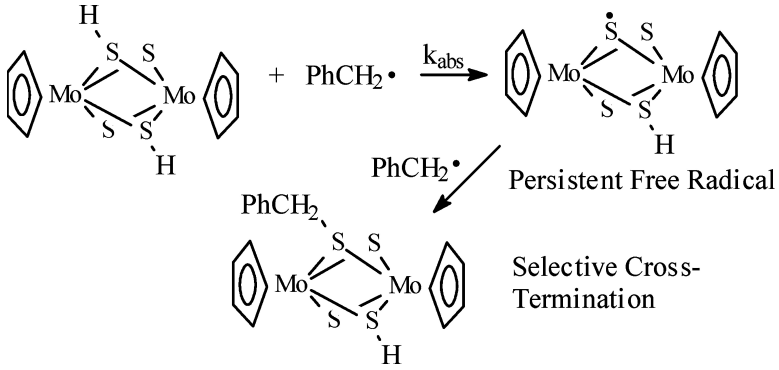

More About This Article

Additional resources and features associated with this article are available within the HTML version:

- Supporting Information
- Links to the 2 articles that cite this article, as of the time of this article download
- Access to high resolution figures
- Links to articles and content related to this article
- Copyright permission to reproduce figures and/or text from this article

View the Full Text HTML

J|A|C|S
ARTICLES
Published on Web 05/08/2004

Activation of the Sulfhydryl Group by Mo Centers: Kinetics of Reaction of Benzyl Radical with a Binuclear Mo(μ-SH)Mo Complex and with Arene and Alkane Thiols

James A. Franz,* Jerome C. Birnbaum,* Douglas S. Kolwaite, John C. Linehan, Donald M. Camaioni, and Michel Dupuis

Contribution from The Pacific Northwest National Laboratory, P.O. Box 999, Richland, Washington 99352

Received February 6, 2004; E-mail: james.franz@pnl.gov; jerome.birnbaum@pnl.gov

Abstract: This paper provides evidence from kinetic experiments and electronic structure calculations of a significantly reduced S−H bond strength in the Mo(μ-SH)Mo function in the homogeneous catalyst model, CpMo(μ-S)$_2$(μ-SH)$_2$MoCp (**1**, Cp = η^5-cyclopentadienyl). The reactivity of **1** was explored by determination of a rate expression for hydrogen atom abstraction by benzyl radical from **1** ($\log(k_{abs}/M^{-1}\ s^{-1}) = (9.07 \pm 0.38) - (3.62 \pm 0.58)/\theta$) for comparison with expressions for $CH_3(CH_2)_7SH$, $\log(k_{abs}/M^{-1}\ s^{-1}) = (7.88 \pm 0.35) - (4.64 \pm 0.54)/\theta$, and for 2-mercaptonaphthalene, $\log(k_{abs}/M^{-1}\ s^{-1}) = (8.21 \pm 0.17) - (4.24 \pm 0.26)/\theta$ ($\theta = 2.303RT$ kcal/mol, 2σ error). The rate constant for hydrogen atom abstraction at 298 K by benzyl radical from **1** is 2 orders of magnitude greater than that from 1-octanethiol, resulting from the predicted (DFT) S−H bond strength of **1** of 73 kcal/mol. The radical CpMo(μ-S)$_3$(μ-SH)MoCp, **2**, is revealed, from the properties of slow self-reaction, and exclusive cross-combination with reactive benzyl radical, to be a persistent free radical.

Introduction

Promoted heterogeneous molybdenum sulfide catalysts are among the most important industrial catalysts, because of their role in hydrodesulfurization (HDS) of petroleum feedstock.[1] MoS clusters are found in oxidase, reductase, dehydrogenase, and nitrogenase enzymes.[2] The chemistry of soluble metal sulfides is recognized to be central to the understanding of the function of bio-organometallic reaction centers in broad categories of enzymatic transformations.[3] Molybdenum-complexed sulfhydryl species play an important role in heterogeneous catalysis in hydrocarbon conversion processes. Much interest continues to surround the development of detailed understanding of molecular-level mechanistic chemistry of promoted Mo_2S_4 systems in hydrogenolysis and hydrodesulfurization (HDS) and in C−S and C−H bond activation. The properties of the S−H and S−C bonds in the Mo−(μ-SR)−Mo group (R = H,C) and in mixed metal (Mo, Co, Ni) μ_2-SR and in μ_3-SR sulfide systems control the activation of S−C bonds in HDS and control catalytic pathways of hydrogenation. The μ-S and μ-SH structures may participate in dihydrogen activation, as depicted in Scheme 1. Recent theoretical studies[4] have reviewed current structural understanding of HDS catalysis and have defined the thermodynamics of hydrogenation of various functional groups of Mo_2S_4. Studies of homogeneous models of CoMoS catalysts have identified mixed metal systems that, most remarkably, may lead to the reduction of S−H and S−aryl bond strengths to as low as 20 kcal/mol.[5] The reduction of S−H and S−C bond strengths in complexes of organosulfur compounds at CoMoS clusters provides efficient pathways both for C−S bond scission (HDS) and for efficient reverse-radical-disproportionation-based hydrogenation (k_{RRD}, Scheme 1) and C−C bond hydrogenolysis. Radical-forming reactions involving hydrogen atom transfer from metal-complexed sulfhydryl groups to unsaturated hydrocarbons may involve both μ- and σ-bonded sulfhydryl groups.

Scheme 1. Dihydrogen Activation and Catalytic Homolytic Pathways in Hydrogenation of Olefins and Dehydrogenation of Saturated Hydrocarbons Involving Mo_nS_{2n} Clusters

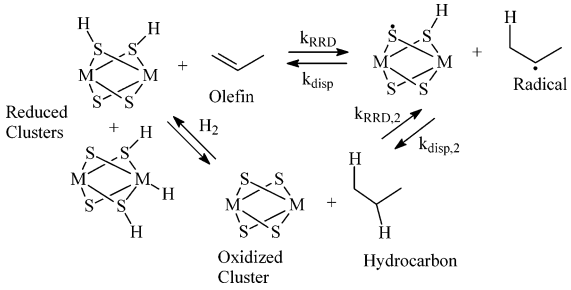

(1) (a) Whitehurst, *Adv. Catal.* **1998**, *42*, 345 and references therein. (b) *Transition Metal-Sulfur Chemistry*; Stiefel, E. I., Matsumoto, K., Eds.; ACS Symposium Series 653; American Chemical Society: Washington, DC, 1996. (c) Topsøe, H.; Clausen, B. S.; Massoth, F. E. In *Catalysis, Science and Technology*; Anderson, J. R., Boudart, M., Ed.; Hydrotreating Catalysis, Science and Technology, Vol. 11; Sprinter Verlag: Berlin, 1996.
(2) *Molybdenum Enzymes, Cofactors, and Model System*; Stiefel, E. I., Coucouvanis, D., Newton, W. E., Eds.; ACS Symposium Series 535; American Chemical Society: Washington, DC, 1993.
(3) Rauchfuss, T. B. *Inorg Chem.* **2004**, *43*, 14−26.
(4) Travert, A.; Nakamura, H.; van Santen, R. A.; Cristol, S.; Paul. J.-F.; Payen, E. *J. Am. Chem. Soc.* **2002**, *124*, 7084−7095.
(5) Curtis, M. D. Hydrodesulfurization Catalysis and Catalyst Models Based on Mo-Co-S Clusters and Exfoliated MoS_2. In *Transition Metal-Sulfur Chemistry*; Stiefel, E. I., Matsumoto, K., Eds.; ACS Symposium Series 653; American Chemical Society: Washington, DC, 1996; pp 154−175.

10.1021/ja049321r CCC: $27.50

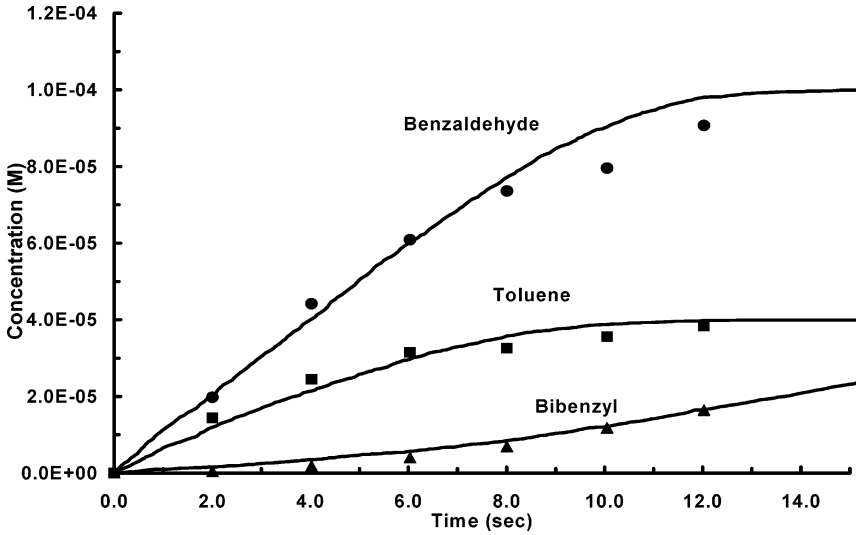

Figure 1. Evolution of products during photolysis of a 0.02 M solution of phenylbenzyl ketone (PBK) in benzene at 315 K in the presence of [CpMo(μ-S)(μ-SH)]$_2$, **1**, 1.4×10^{-4} M. Product evolution is depicted for benzaldehyde (●), toluene (■), and bibenzyl (▲). The rate constant for abstraction of a hydrogen atom from **1** by benzyl radical, $k_{abs} = 3.4 \times 10^6$ M^{-1} s^{-1}, was determined using data at 2.0 s (eq 10a). The solid lines are predicted concentrations of benzaldehyde, toluene, and bibenzyl found by numerical integration of the equations of Scheme 2, employing a rate of photolysis of PBK, 5.7×10^{-6} M/s, and $k_4 = 0.5(k_5 + k_6) = 0.5(k_7 + k_8) = 2.2 \times 10^9$ and $k_9 = 4.4$, 4.4, and 2.2×10^9 M^{-1} s^{-1}, respectively. Fits of depicted data are sensitive to the choice of k_4 but insensitive to the choice of k_5 and k_6, and equivalent fits are obtained with low termination rates for **2**, e.g., $<10^4$ M^{-1} s^{-1}. The rate constant for abstraction of hydrogen by benzoyl radical (PhCO•) from **1**, 3×10^7 M^{-1} s^{-1}, was found by variation of rate constants to optimize the fit of the above data to numerical integration of eqs 1−9 (Scheme 2) subject to the constraints listed above. Convenient programs are available for numerical integration and optimization.[16]

The role of reverse-radical-disproportionation (k_{RRD} and k_{RRD2} depicted in Scheme 1) is now well-established in radical initiation[6] and hydrogenation pathways, as well as in controlled polymerization.[7] The rate of radical initiation via RRD is directly dependent on $\Delta H°_{RRD}$ or $\Delta H°_{init}$ (cf. Scheme 1) and in turn on the M−H or S−H (M = Co, Mo, Ni) bond strengths of the hydrogen atom donors. The underlying thermochemistry of S−H bonds of μ-SH bridges between Mo atoms or Mo and Co or Ni atoms remains largely unexplored. No direct measure of homolytic reactivity of the μ_2-SH or μ_3-SH structures has been reported, nor have S−H bond strengths been measured for MoS or MoCoS clusters that are models for activation of S−H and C−S bonds important to catalysis. A more detailed knowledge of homolytic reactivity and thermochemistry of the μ-S and μ-SH groups is desirable for understanding stepwise catalytic transformations involving C−S and S−H bond activation.

The novel reactivity of bridging μ-S groups in hydrogen activation, catalytic hydrogenation, and bond formation involving olefins, acetylenes, and alkyl functionality was early recognized by M. Rakowski-DuBois and co-workers. The soluble binuclear species [CpMo(μ-S)(μ-SH)]$_2$, **1**, and related species have been the subject of considerable interest, because of the relationship of the patterns of reactivity of the embedded Mo_2S_4 cluster to key heterogeneous catalytic reaction steps of MoS and promoted catalysts.[8] The complex **1** contains two bridging hydrosulfido ligands and two bridging sulfur atoms.

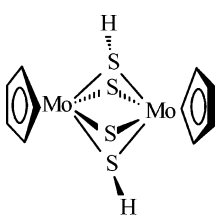

1

Complex **1** catalyzes HD formation from mixtures of H_2/D_2 or H_2/D_2O, demonstrating that the complexed hydrosulfido group has the ability to activate dihydrogen as well as engaging in acid−base equilibria with Brønsted acids. Extended Hückel calculations revealed the bridging sulfur atoms to exhibit HOMO and LUMO orbitals with proper symmetry to confer donor and acceptor properties to the sulfur bridge atoms similar to those associated with a transition metal.[9] The complex reacts directly with olefins and acetylenes, displacing dihydrogen from the sulfhydryl groups by olefins and acetylenes to form bridging bis-alkyl- or bis-alkenyl-dithiolate complexes, respectively.[8] The characteristic of the Mo_2S_4 cluster of **1** to activate H_2 and to react directly with olefins reflects the novel reactivity available to the μ_2-S functional groups of the cluster. In previous work, we examined hydrogen transfer from thiols to carbon-centered radicals and to thiyl radicals, supporting quantitative mechanistic studies using hydrogen atom transfer from thiols as basis rate standards.[10] The present work extends those studies to systems of catalytic interest. Although wide interest persists in molybdenum hydride and molybdenum-sulfhydryl systems,[11] only a

(6) Rüchardt, C.; Gerst, M.; Ebenhoch, J. *Angew. Chem., Int. Ed. Engl.* **1997**, *36*, 1406.
(7) Tang, L.; Papish, E. T.; Abramo, G. P.; Norton, J. R.; Baik, M.-H.; Friesner, R. A.; Rappe, A. *J. Am. Chem. Soc.* **2003**, *125*, 10093−10102 and references therein.
(8) Rakowski DuBois, M.; VanDerveer, M. C.; DuBois, D. L.; Haltiwanger, R. C.; Miller, W. K. *J. Am. Chem. Soc.*, **1980**, *102*, 7456.
(9) DuBois, D. L.; Miller, W. K.; Rakowski DuBois, M. *J. Am. Chem. Soc.* **1981**, *103*, 3429.
(10) (a) Franz, J. A.; Bushaw, B. A.; Alnajjar, M. S. *J. Am. Chem. Soc.* **1989**, *111*, 268. (b) Alnajjar, M. S.; Garrossian, M. S.; Autrey, S. T.; Ferris, K. F.; Franz, J. A. *J. Phys. Chem.* **1992**, *96*, 7037.
(11) Examples include: (a) Rakowski DuBois, M. Catalysis by Sulfido Bridged Dimolybdenum Complexes. In *Catalysis by Di-and Polynuclear Metal Cluster Complexes*; Adams, R. D., Cotton, F. A., Eds.; Wiley-VCH Inc.: New York, 1998; pp 127−143 and references therein. (b) Reference 4. (c) Sarker, N.; Bruno, J. W. *J. Am. Chem. Soc.* **1999**, *121*, 2174. (d) Fettinger, J. C.; Kraatz, H. B.; Poli, R.; Quadrelli, E. A.; Torralba, R. C. *Organometallics* **1998**, *17*, 5767. (d) Bayse, C. A.; Hall, M. B.; Pleune, B.; Poli, R. *Organometallics* **1998**, *17*, 4309. (e) Hascall, T.; Murphy, V. J.; Parkin, G. *Organometallics* **1996**, *15*, 3910. (f) Tsai, Y. C.; Johnson, M. J. A.;

Scheme 2. Kinetic Steps in the Steady-State Photolysis of Phenylbenzyl Ketone (PBK) in the Presence of $[CpMo(\mu\text{-}S)(\mu\text{-}SH)]_2$ (**1**)

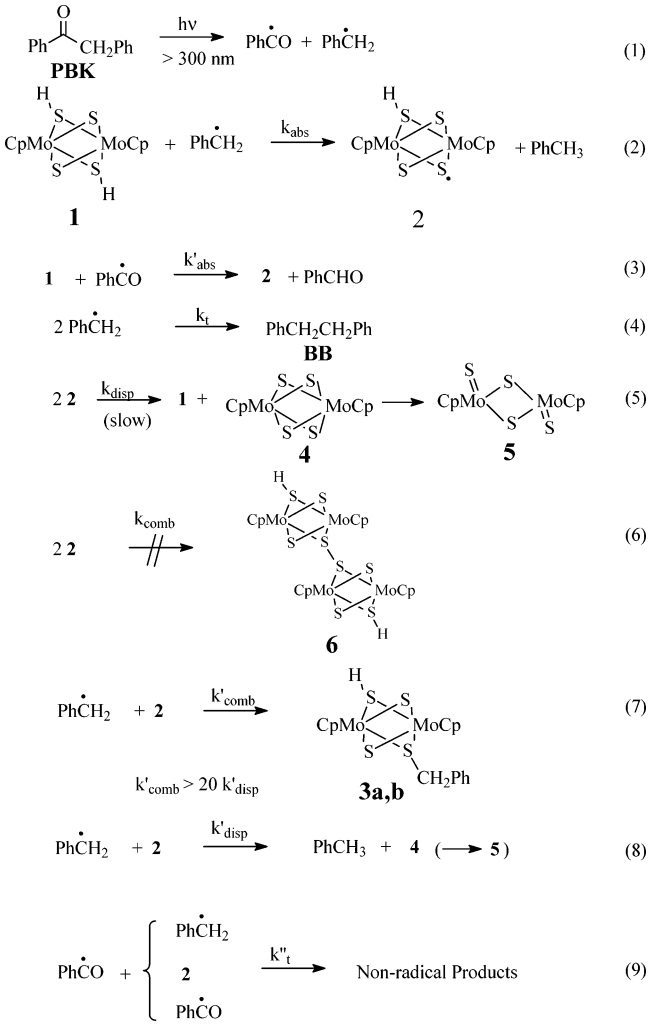

few kinetic studies have been carried out involving hydrogen atom transfer from molybdenum hydrides,[12,13] along with several measurements of Mo−H bond strengths.[14] We present a kinetic characterization of the activation of the Mo−(μ-SH)−Mo group in the $Mo_2S_4H_2$ cluster, **1**, along with estimates of the Mo(μ-SH)Mo S−H bond strength based on a correlation of abstraction rates with rate constants for reactions of carbon-centered radicals with thiols and DFT bond dissociation enthalpy calculations comparing the S−H bond strength of **1** with arene and alkane thiols and H_2S. New rate expressions for reaction with benzyl radical with alkane and aryl thiols are presented for comparison to the reactivity of the MoSH cluster.[13,15] Evidence is presented showing that the radical $CpMo(\mu\text{-}S)_2(\mu\text{-}SH)(\mu\text{-}S^{\bullet})MoCp$, **2**, formed from hydrogen atom abstraction from **1**, does not undergo self-reaction to form a dimer but predominately undergoes cross-termination with a benzyl radical to give the isomeric cross-termination product $CpMo(\mu\text{-}SCH_2Ph)(\mu\text{-}S)_2(\mu\text{-}SH)MoCp$ (**3a**,**b**). Evidence suggests that radical **2** does not form a dimer and undergoes self-reaction exclusively, and very slowly, by disproportionation, possibly forming transient $CpMo(\mu\text{-}S)_4MoCp$ (**4**), which forms the thermodynamically favored rearrangement product **5** ($CpMo(=S)(\mu\text{-}S)_2Mo(=S)Cp$) (Scheme 2). The slow self-disproportionation of **2**, taken with the selective cross-combination of **2** with transient radicals (benzyl), demonstrates that **2** is a persistent free radical.

Results

Kinetics of Reaction Benzyl Radical with $[CpMo(\mu\text{-}S)(\mu\text{-}SH)]_2$, 1. Rate constants for hydrogen atom abstraction by the benzyl radical from **1** were determined by a competition of hydrogen atom abstraction by benzyl radical to form toluene with benzyl radical self-termination to produce bibenzyl during photolysis of phenylbenzyl ketone (PBK) or dibenzyl ketone (DBK) in benzene solutions. The benzyl radical was produced by broadband visible UV irradiation (>330 nm) of optically dilute solutions of phenylbenzyl ketone (PBK) and **1**.

Under conditions of constant rate of photolysis of phenylbenzyl ketone and a short extent of conversion of the hydrogen donor, typically less than 5−7%, the relationship among toluene, bibenzyl (BB), and the average hydrogen atom donor concentration is given by eq 10a, where $[DH]_{av}$ is the average concentration of the thiol donor over a period of photolysis time, Δt:

$$k_{abs} = \frac{[\text{Toluene}]k_t^{1/2}}{[\text{BB}]^{1/2}[\text{DH}]_{av}\Delta t^{1/2}} \qquad (10a)$$

$$[\text{Toluene}] = [\text{DH}]_0(1 - e^{-k_{abs}[BB]^{1/2}\Delta_t^{1/2}/k_t^{1/2}}) \qquad (10b)$$

In practice, conversion of donor (**1**) up to 50% leads to less than 20% error in rate constant k_{abs} using eq 10a. An integrated rate equation, eq 10b, may be applied for the case of extensive conversion of starting donor at constant rate of photolysis of PBK or DBK. For the PBK experiments, the yields of benzaldehyde and toluene were used to calculate the average concentration of hydrogen donor consumed. Combining experimental values of bibenzyl and toluene at each photolysis time (0.5−8.0 s) with the rate constant for self-termination of bibenzyl, k_t (see below), provides values of k_{abs} at each temperature. The rate of photolysis of PBK employed in the kinetic measurements was approximately $(3-7) \times 10^{-7}$ M s^{-1}, corresponding to a steady-state concentration of benzyl radical of about 2×10^{-8} M. The rate of formation of toluene and bibenzyl was found to be linear during the first several seconds of photolysis, justifying the use of eq 10a for calculation of rate constants. The resulting temperature-dependent rate constants for the reaction of benzyl radical with $[CpMo(\mu\text{-}S)(\mu\text{-}SH)]_2$ are shown in Figure 2, and the rate expression is presented in Table 1.

Hydrogen Abstraction by Benzyl Radical from 1-Octanethiol in Benzene and Cyclohexane. Rate constants for

Mindiola, D. J.; Cummins, C. C. *J. Am. Chem. Soc.* **1999**, *121*, 10426. (g) Nolan, S. P.; Lopez de la Vega, R.; Hoff, C. D. *J. Organomet. Chem.* **1986**, *315*, 187. (h) Hoff, C. D. *J. Organomet. Chem.* **1985**, *282*, 201. (i) Landrum, J. T.; Hoff, C. D. *J. Organomet. Chem.* **1985**, *282*, 215.
(12) (a) Eisenberg, D. C.; Norton, J. R. *Isr. J. Chem.* **1991**, *31*, 55. (b) Eisenberg, D. C.; Lawrie, C. J. C.; Moody, A. E.; Norton, J. R. *J. Am. Chem. Soc.* **1991**, *113*, 4888.
(13) Franz, J. A.; Linehan, J. C.; Birnbaum, J. C.; Hicks, K. W.; Alnajjar, M. S. *J. Am. Chem. Soc.* **1999**, *121*, 9824.
(14) (a) Tilset, M.; Parker, V. D. *J. Am. Chem. Soc.* **1989**, *111*, 6711. (See also Additions and Corrections. *J. Am. Chem. Soc.* **1990**, *112*, 2843.) (b) Reference 11g.
(15) Franz, J. A.; Naushadali, S. K.; Alnajjar, M. S. *J. Org. Chem.*, **1986**, *51*, 19.
(16) (a) Macey, R. I.; Oster, G. F. *Berkeley Madonna*, version 8.0.1; 2000. See: http://www.berkeleymadonna.com/. (b) Hinsberg, W.; Houle, F.; Allen, F.; Yoon, E. *Chemical Kinetics Simulator*, v. 101; IBM Almaden Research Center. See: https://www.almaden.ibm.com/st/computational_science/ck/msim/.

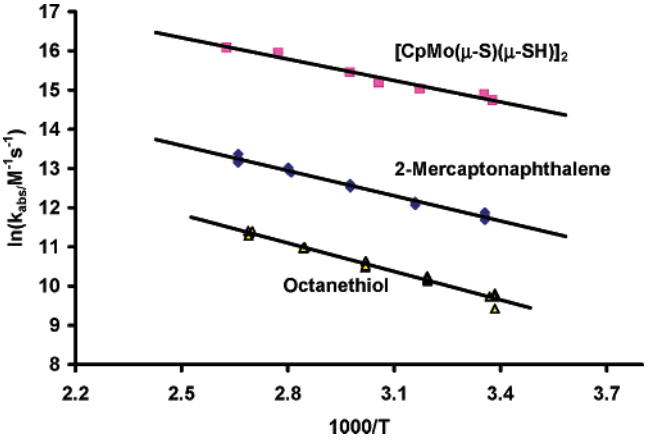

Figure 2. Temperature-dependent rate data for abstraction of hydrogen atom by benzyl radical from $[CpMo(\mu\text{-}S)(\mu\text{-}SH)]_2$ (**1**), 2-mercaptonaphthalene, and octanethiol in benzene.

Scheme 3

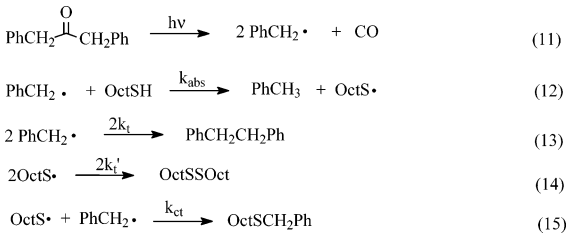

hydrogen abstraction by benzyl radical from 1-octanethiol were determined in competition experiments by steady-state photolysis of dibenzyl ketone (DBK) in benzene solutions and in cyclohexane solutions. Benzyl radical was produced by broadband visible UV irradiation (>330 nm) of optically dilute solutions of DBK and 1-octanethiol, as shown in Scheme 3. Under the conditions employed, the relationship among toluene, bibenzyl, and the average donor concentration, $[DH_{av}]$, is given by eq 10a. In typical experiments, less than 6% of the donor was consumed. The rate of photolysis of DBK employed in the kinetic measurements was about 2×10^{-6} M s^{-1}, corresponding to a steady-state concentration of benzyl radical of about 1×10^{-7} M. The yield of toluene was used to calculate an average thiol concentration during the photolysis. The temperature-dependent plot of data for the reaction of benzyl radical with 1-octanethiol is shown in Figure 2, covering a range of 295−374 K, and the rate expression is presented in Table 1. Kinetics of reaction of benzyl radical were also carried out in cyclohexane for comparison with benzene, to rule out formation of a portion of the product toluene by reaction of benzyl radical with octanethiylcyclohexadienyl radical, the adduct of 1-octanethiyl radical to the solvent. This would potentially react with benzyl radical to give toluene and octylphenylsulfide. In experiments with benzene employing extended photolysis times (>60 s), octylphenylsulfide was detectable by GC/MS. However, at photolysis times (<5 s) used in kinetic measurements, the sulfide was not detectable and kinetics carried out in cyclohexane yielded Arrhenius rate parameters close to those obtained in benzene, $[\log(k_{abs}/M^{-1}\ s^{-1}) = (7.75 \pm 0.21) - (4.79 \pm 0.31)/\theta$, ($\theta = 2.303RT$ kcal/mol, errors are 2σ)]. The participation of

Table 1. Rate Parameters for the Reaction of Benzyl Radical with a μ-SH Complexed Molybdenum Thiol **1**, Arene and Alkane Thiols, and a Molybdenum Hydride (Errors Are 2σ)

hydrogen donor	X–H BDE (kcal/mol)	log A (M^{-1} 's^{-1})	$\Delta S^{\ddagger}$ (eu) (T_m, K)	E_a[h] (kcal/mol)	$\Delta H^{\ddagger}$ (kcal/mol)	k ($M^{-1}s^{-1}$) 298 K	mean temp (T_m, K)	temp range (K)
$[CpMo(\mu\text{-}S)(\mu\text{-}SH)]_2$[b]	73(calcd)[e]	9.07 ± 0.38	−19.2 ± 1.8	3.62 ± 0.58	2.96 ± 0.58	2.6×10^6	331	295−372
$C_{10}H_7$-2-SH[b,d]	77.9[g]	8.21 ± 0.17	−23.2 ± 0.8	4.24 ± 0.26	3.57 ± 0.26	1.3×10^5	337	298−376
$CH_3(CH_2)_7SH$[b]	87.3[g]	7.89 ± 0.35	−24.7 ± 1.6	4.64 ± 0.54	3.96 ± 0.54	3.1×10^4	341	295−374
$CH_3(CH_2)_7SH$[c]	87.3[g]	7.75 ± 0.21	−25.3 ± 1.0	4.79 ± 0.31	4.12 ± 0.31	1.7×10^4	333	295−372
$Cp^*Mo(CO)_3H$[a,b,f]	70[a]	8.89 ± 0.22	−20.0 ± 1.0	2.31 ± 0.33	1.66 ± 0.33	1.6×10^7	325	297−373

[a] Nolan, S. P.; Vega, R. L.; Hoff, C. D. *Organometallics* **1986**, *5*, 2529−2537. Tilset, M.; Parker, V. D. *J. Am. Chem. Soc.* **1989**, *111*, 6711−6717. See Additions and Corrections, *J. Am. Chem. Soc.* **1990**, *112*, 2843. [b] Solvent, benzene. [c] Solvent, cyclohexane. [d] 2-Mercaptonaphthalene. [e] Estimated from DFT bond dissociation isodesmic calculations, this work; see text. [f] Cp* = pentamethyl-η^5-cyclopentadienyl. [g] Reference 34. Bordwell, F. G.; Zhang, X.-M.; Satish, A. V.; Cheng, J. P. *J. Am. Chem. Soc.* **1994**, *116*, 6605. [h] A = Arrhenius preexponential factor, Ea = Arrhenius exponential constant in $k = Ae^{-E_a/RT}$.

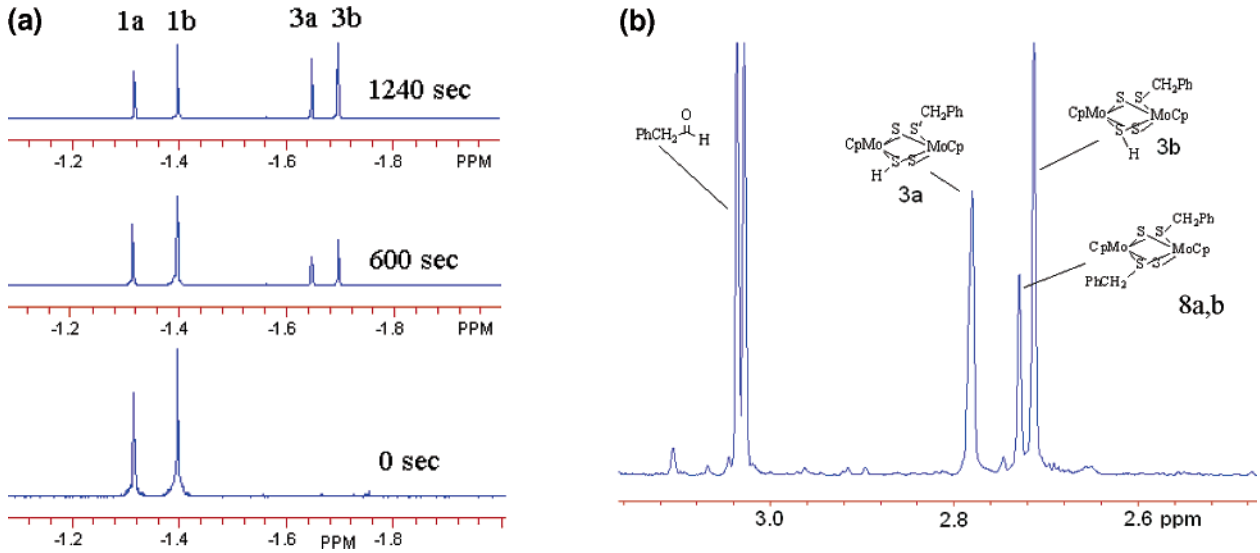

Figure 3. (a) ^{1}H NMR spectra of photolysis of DBK and **1**. (b) ^{1}H NMR spectrum of photolysis of DBK and **1**, 3000 s.

Scheme 4. Photolysis of DBK in the Presence of **1** Yields Predominately **3a**,**b** and Trace Amounts of **5**; See Text[a]

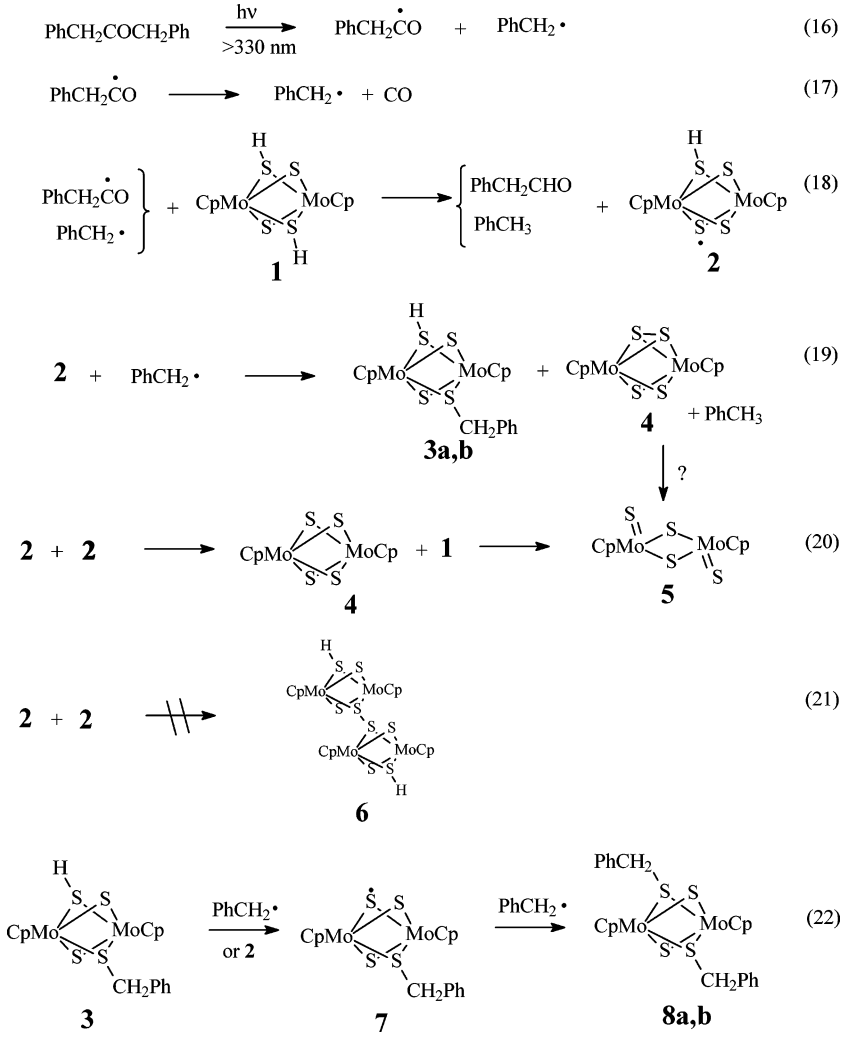

[a] Compounds **5** and **6** are not detected. Benzyl radical undergoes nearly exclusive combination with **2** to form **3**.

the addition/cross-termination pathway in production of toluene appears negligible.

Hydrogen Abstraction by Benzyl Radical from 2-Mercaptonaphthalene. Kinetics of reaction of benzyl radical with 2-mercaptonaphthalene were determined in benzene under conditions employed for octanethiol. Temperature-dependent rate data are depicted in Figure 2 and presented in Table 1.

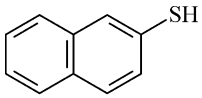

2-Mercapto-naphthalene

Slow Self-Reaction of 2 and Dominant Cross-Termination of 2 with Benzyl Radical. The photolysis of dibenzyl ketone was carried out in the presence of a higher concentration of **1**, 0.0005 M, than employed in the kinetic experiments, to facilitate the observation of photoproducts derived from **2** and benzyl radical by ^{1}H NMR. The photoconversion steps are described in eqs 16−22. Figure 3a shows the consumption of the two isomers of **1** and the appearance of a new pair of hydride resonances at −1.64 and −1.7 ppm in $CDCl_3$. The new hydride peaks are accompanied by the appearance of two new benzylic CH_2 resonances (Figure 3b) at 2.70 and 2.78 ppm exhibiting twice the integrated intensity of the hydride resonances. The resonances at 2.7 and 2.8 ppm are assigned to the cross-termination product isomers **3a** and **3b**. (Note phenylacetaldehyde formed by trapping by **1** of the intermediate phenylacetyl radical.) Under conditions of extensive conversion, **3a** and **3b** are further converted to the dibenzyl substituted cluster **8**. To aid in the identification of isomers of **3** and **8**, hydride **1** was subject to exchange of μ_2-SH groups with benzylthiol (eq 23):

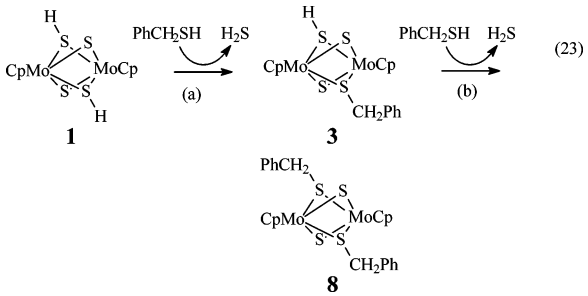

Exchange of benzylthiol with **1** provided two products, **3a** and **3b**, with ^{13}C and ^{1}H NMR spectra identical to those produced in the photolysis experiments, followed by further conversion of isomers **3** to **8**. The exchange reaction, eq 23,

Table 2. ^{13}C and ^{1}H Data for Isomers of **1**, **3**, **5**, and **8**

compound	solvent	^{1}H NMR data	^{13}C NMR data
1a	$CDCl_3$	6.37(10H,s), −1.41 (1H,s)	98.07
1b	$CDCl_3$	6.37(10H,s), −1.48 (1H,s)	98.15
1a	benzene-d_6	5.89 (10H,s), −1.32 (1H, s)	
1b	benzene-d_6	5.89 (10H,s), −1.40 (1H,s)	
3a	$CDCl_3$	6.22(10H,s), 2.80(2H,s), −1.78(1H,s)	141.35,128.89(2C),128.23(2C), 126.85, 98.07(10C), 44.52
3b	$CDCl_3$	6.23(10H,s), 2.74(2H,s), −1.86(1H,s)	140.56, 129.05(2C), 128.45(2C), 126.83, 98.05(10C), 43.49
3a	benzene-d_6	5.87(10H,s), 2.78(2H,s), −1.65(1H,s)	
3b	benzene-d_6	5.87(10H,s), 2.71(2H,s), −1.70(1H,s)	
5	benzene-d_6	5.78 (10H, s)	
5	$CDCl_3$	6.34 (10H, s)	
8a	$CDCl_3$	7.23(6H,m), 6.86(4H,m), 6.08(10H,s), 2.764(4H,s)	141.2(2C), 129.05(4C), 128.41(4C), 126.74(2C), 98.16(10C), 42.09
8b	$CDCl_3$	7.21(6H,m), 6.84(4H,m), 6.13(10H,s), 2.712(4H,s)	140.71(2C), 129.23(4C), 128.37(4C), 126.62(2C), 98.11(10C), 38.10
8a	benzene-d_6	7.2(6H,m), 6.8(4H,m), 5.85(10H,s), 2.73(4H,s)	

was found to proceed much more rapidly in $CDCl_3$ than in benzene-d_6, and the second step (eq 23b) was found to be appreciably faster than the initial step (eq 23a). Preparative column chromatography of the exchange mixture containing **1**, **3**, and **8** on alumina (eluent, CH_2Cl_2) led to nearly pure isomers of **8** that were found to be conformationally stable. Similar to **1**, the isomers of **3** are always found in the same ratio, reflecting a facile acid/base-catalyzed pathway available to the SH protons that retains the equilibrium mixture of **3a** and **3b**. (Note that the assignment of isomeric structures remains (**3a** vs **3b** and **8a** vs **8b**) ambiguous.)

Traces of the disproportionation product assigned as **5** were identified by prompt (within 10 min) ^{1}H NMR spectroscopy of the product mixture from photolysis of DBK in the presence of **1** in benzene-d_6. The product **5** was present at less than 5% of the concentration of **3a**,**b**. No ^{1}H NMR transitions attributable to **6** were detectable among the photoproducts. (Isomers of **6** are expected to give at least two unique SH protons in the range −1 to −3 ppm.) Although radical **2** is predicted in kinetic modeling to be present at significant steady-state population and would be expected to undergo self-reaction to form **4** (or **5**) or **6** (see e.g., Scheme 4), no new hydride resonances attributable to **6** in the ^{1}H NMR spectrum were detectable, and **5** was shown to be transient in solution due to extremely low solubility in $CDCl_3$ and benzene-d_6 (see below). Although self-termination product **6** was not detected in the present experiments, formation of a disulfide linkage between Mo_2S_4 binuclear units is well-known.[17] The present experiments do not rule out the formation of **6** followed by *rapid* decomposition of **6** to give **1** and **5**, e.g., equivalent to the self-disproportionation products of radical **2**.

However, in promptly examined experiments in which DBK was photolyzed in the presence of **1**, no more than trace amounts of **4** or **5** were formed. Thus, **4** and/or **5** are not formed by cross-disproportionation of benzyl radical and **2** or by self-disproportion of **2**, competitive with cross-combination of benzyl radical with **2**. Table 2 presents NMR data for **1**, the structure assigned as **5**, and isomers of **3** and **8**.

$$Bu_tOOBu_t \xrightarrow{h\nu} Bu_tO^{\bullet} \tag{24}$$

$$Bu_tO^{\bullet} + \mathbf{1} \xrightarrow{k_{abs''}} Bu_tOH + \mathbf{2} \tag{25}$$

$$2\,\mathbf{2} \xrightarrow{k_{disp}} \mathbf{1} + Cp_2Mo_2(S)_4\ (\mathbf{4}\text{ and/or }\mathbf{5}) \tag{26}$$

$$2\,\mathbf{2} \xrightarrow{k_{comb}} \mathbf{6} \xrightarrow{k_{dec}} \mathbf{1} + (\mathbf{4}\text{ and/or }\mathbf{5}) \tag{27}$$

$$Cp_2Mo_2(S)_4\ (\mathbf{4}) \rightarrow \mathbf{5} \tag{28}$$

$$Cp_2Mo_2(S)_4\ (\mathbf{4}\text{ and/or }\mathbf{5}) \rightarrow \text{precipitate} \tag{29}$$

Formation of Disproportionation Product 5. The lack of formation of **6** via dimerization of **2** in the photochemical experiments above involving reactions of benzyl radical and **2**, together with the predominance of products **3a**,**b**, raises the question of whether **2** participates in slow self-*disproportionation* to form **4** and/or **5** *in the absence of reactive radicals* such as benzyl. To observe self-reaction of radical **2** in the absence of reactive alkyl radicals, **2** was produced by reaction of a *tert*-butoxyl radical with **1**. Thus, freeze−thaw degassed solutions of **1** and di-*tert*-butylperoxide in benzene-d_6 were photolyzed with the diffuse beam of a 1-kW high pressure xenon arc lamp and promptly examined by ^{1}H NMR spectroscopy over the time period 5−90 min. Approximately 25% of **1** was cleanly converted to a new Cp resonance at 5.78 ppm, which disappeared (by precipitation) with a half-life of 120 min at 298 K. No new S−H resonances in the region −1 to −3 ppm, corresponding to cross-termination or self-termination products from **2**, were observed. Because of the very high expected rate of reaction of *tert*-butoxyl radical with **1** ($5-10 \times 10^8$ M^{-1} s^{-1}), *tert*-butoxyl radical is entirely consumed in abstraction (eq 25), to the exclusion of cross-termination reactions with **2** (and unlike experiments in which benzyl radical undergoes appreciable cross-termination with **2** during the steady-state photolysis of DBK). Thus, **2** reacts slowly by self-reaction (eqs 26, 27). The absence of new SH resonances attributable to **6** suggests that **5** can form by a slow, *apparent* disproportionation of **2** (eq 26). An alternative pathway that cannot be formally

(17) (a) Birnbaum, J. C.; Godziela, G.; Maciejewski, M.; Tonker, T. L.; Haltiwanger, R. C.; Rakowski DuBois, M. *Organometallics* **1990**, *9*, 394. (b) Birnbaum, J. C.; Laurie, J. C. V.; Rakowski DuBois, M. *Organometallics* **1990**, *9*, 156.

ruled out involves the formation of **6** by dimerization of **2**, followed by *rapid* decomposition of **6** to **1** and insoluble **5** (eq 27). The transient ^{1}H NMR peak observed at 5.89 ppm is assigned to **5**, the disproportionation product of **2**.

A. Assignment of Product of Oxidation of 1 to Structure 5. Assignment of the observed transient species to **5** is based on the observation of a strong M═S stretch observed in the FTIR spectrum of the solid product isolated from the reaction of azo-benzene and **1**: the dark solid exhibited absorptions (KBr pellet) at 523 (w), 481 (s), 432 (m), and 406 (m) cm^{-1}, respectively, assigned to $\nu_{Mo=S}$, $\nu'_{Mo=S}$, $\nu_{Mo-S-Mo}$ and $\nu'_{Mo-S-Mo}$ frequencies, respectively. Candidate structures for oxidation product(s) of **1** include **4**, **5**, **9** (the syn-isomer of **5**), and **10**, with relative energies depicted for **4**, **5**, and **9** (0 K B3LYP DFT energies and geometries calculated with a hybrid basis set consisting of LANL2DZ ECP at Mo and 6-31G(d) at C,H, and S). Brunner et al.[18] proposed a structure for an isomer of

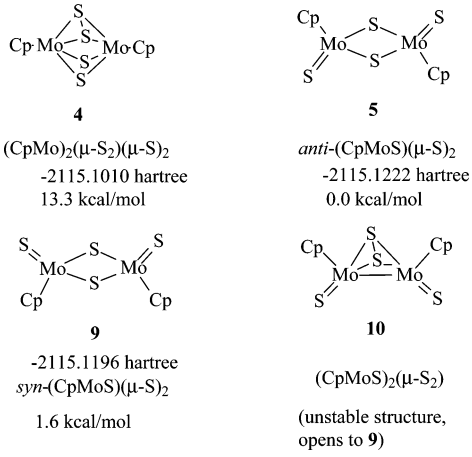

the formula Cp*$_2$Mo$_2$S$_4$ (Cp* = η^5-C$_5$ (CH$_3$)$_5$) to be (Cp*MoS)$_2$-(μ-S$_2$), analogous to **10**. An X-ray crystal structure was not available to verify the structure. While the structures **4**, **5**, and **9** were readily located in DFT calculations in this work, all attempts to locate a stable structure corresponding to **10** failed, with the initial structures of **10** opening during geometry optimization to form **9** (relative energies shown).

The syn-isomer **9** is predicted to lie 1.6 kcal/mol higher in energy than anti-isomer **5**. A strong frequency observed at 481 cm^{-1} (Mo═S) suggests **5** or **9** to be likely, with **10** ruled out as a candidate. From computational results suggesting **5** to be most stable, we have selected **5** as the most probable candidate. This assignment does not rule out the possibility of initial formation of **4**, either in *azo*-benzene oxidation of **1** or in the photochemical free radical oxidation of **1** by benzyl or *tert*-butoxyl radicals, followed by thermal or photoinduced conversion of **4** to **5** in the present experiments.

While an early report of the preparation of **5**[19] was found to be problematic,[20] both [Cp′MoS(μ-S)]$_2$ (**11**, Cp′ = MeCp) and [Cp*MoS(μ-S)]$_2$ (**12**, Cp* = pentamethyl-η^5-cyclopentadienyl) have been prepared[21] in high yields from the parent compounds, [Cp′Mo(μ-SH)(μ-S)]$_2$ (**13**) and [Cp*Mo(μ-SH)(μ-S)]$_2$ (**14**), by oxidation with *azo*-benzene, which is reduced to 1,2-diphenylhydrazine. Both **11** and **12** are rapidly reconverted to **13** and **14** by exposure to H_2.[22] In this work, compound **5** was independently prepared by oxidation of **1** with azo-benzene in $CDCl_3$ and benzene-d_6 and *gave an identical Cp chemical shift* and solubility characteristics as those of **5** formed in reactions of **1** in radical reactions of benzyl or *tert*-butoxyl radicals. When **5** was formed by oxidation of **1** with *azo*-benzene, it was also found to be highly insoluble in benzene and $CDCl_3$. Finally, insoluble **5** formed in the *azo*-benzene oxidation reaction was rapidly reconverted to **1**, under 1 atm of H_2 at 60−80 °C. Initial formation of **4** followed by photolytic or thermal conversion to **5** is not ruled out by these results.

Bruce and Tyler[23] reported the photolytic interconversion of **12**, **16**, and **15**, and Brunner et al.[18] reported thermal conversion of **16** to **15**. Based on these reports, conversion of **4** to **5** is expected.[24] Based on our theoretical results, it may be possible that the structure proposed to be **15** is actually the syn-isomer of **12**.

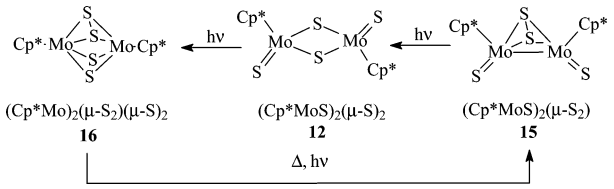

B. Further Evidence for Slow Self-Reaction of 2. An experiment to semiquantitatively estimate the rate of self-termination of **2** was carried out. In an NMR scale photolysis experiment, an oxygen-free solution of DBK (0.015 M) and **1** (0.003 M) in benzene-d_6 was photolyzed with a 1-kW high Xe lamp for 180 s to give toluene (0.004 M) and **3** but no detectable **5**, under conditions of a lower limit of detection of **5** of ~10^{-5} M. From the yield of toluene and the known rate constant, k_{abs} = 2.6 × 10^6 M^{-1} s^{-1} (Table 1), the steady-state benzyl radical concentration is estimated to be [PhCH$_2^\bullet$] ≅ [toluene]/(Δt)(k_{abs})-(2*[**1**]) = [toluene]/(180 s)(2.6 × 10^6)(0.006) =1.4 × 10^{-9} M. Assuming a conventional cross-termination rate constant for the reaction of benzyl radical and **2**, 2 × 10^9 M^{-1} s^{-1}, together with the yield of **3** and the benzyl radical concentration from above, the steady-state concentration of **2** can be estimated from the relation [**2**] ≅ [**3**]/(180 s)([PhCH$_2^\bullet$])(2 × 10^9 M^{-1} s^{-1}) = 3 × 10^{-6} M. Finally, from the relation [**5**]/Δt ≅ k_{disp}[**2**]^2 and an upper limit of [**5**] < 10^{-5} M, a value of k_{disp} < 5 × 10^3 M^{-1} s^{-1}is estimated. The rate constant for self-reaction of **2** is thus at least 10^5-fold slower than normal bimolecular radical termination rates. From the estimates of radical concentrations above, the buildup of a high concentration of the persistent radical (**2**) causes the transient radical (benzyl) to be steered to follow the cross-termination path. The properties of **2** closely reflect the behavior expected for persistent free radicals.[25,26] This is dramatically shown in Figure 3a, which illustrates the clean, exclusive formation of cross-termination products **3a**,**b**.

(18) Brunner, H.; Meier, W.; Wachter, J.; Guggolz, E.; Zahn, T.; Ziegler, M. *Organometallics* **1982**, *1*, 1107−1113.
(19) Beck, W.; Danzer, W.; Thiel, G. *Angew. Chem., Int. Ed. Engl.* **1973**, *12*, 582.
(20) Rakowski DuBois, M.; Haltiwanger, R. C.; Miller, D. J.; Glatzmeier, G. *J. Am. Chem. Soc.* **1979**, *101*, 5245.
(21) Casewit, C. J.; Coons, D. E.; Wright, L. L.; Miller, W. K.; DuBois, M. R. *Organometallics* **1986**, *5*, 951−955.
(22) Rakowski DuBois, M.; DuBois, D. L.; VanDerVeer, M. C.; Haltiwanger, R. C. *Inorg. Chem.* **1981**, *20*, 3064.
(23) Bruce, A. E.; Tyler, D. R. *Inorg. Chem.* **1984**, *23*, 3433−3434.
(24) The authors thank the reviewers for pointing out the possible photolytic interconversion of **4** to **5**.
(25) Fischer, H. *J. Am. Chem. Soc.* **1986**, *108*, 3925.
(26) Karatekin, E.; O'Shaughnessy, B.; Turro, N. J. *J. Chem. Phys.* **1998**, *108*, 9577.

Table 3. Electronic Energies and Total Enthalpy Corrections, 298 K (hartree/particle)

species	LANL2DZ[a]	LANL2DZdp[a]	ELANL2DZ[a]	ECEP-121G[a]	LANL2DZ (6-31G*)[e]	LANL2DZ(6-311++G(2d,dp)[f]	enthalpy correction[g]
H•[b]	−0.498 91[b]	−0.501 94[b]	−0.502 26[b]	−0.502 26[b]			0.00236
HS•	−10.657 75	−10.679 60	−398.774 34	−398.774 34	−398.740 027 8	−398.774 737 2	0.008 80
H_2S	−11.289 78	−11.326 47	−399.425 04	−399.425 04	−399.385 435 5	−399.426 311 3	0.017 76
CH_3S•	−49.973 49	−49.999 76	−438.102 12	−438.102 12	−438.059 669 1	−438.103 971 3	0.040 23
CH_3SH	−50.599 89	−50.640 56	−438.747 09	−438.747 09	−438.698 348 4	−438.748 834 8	0.049 04
PhS•	−241.687 58	−241.763 49	−629.903 56	−629.903 56	−629.809 997 9	−629.906 204 3	0.095 94
PhSH	−242.301 55	−242.391 48	−630.534 64	−630.534 64	−630.434 123	−630.537 837 1	0.104 29
Nap-2-S•[c]	−395.309 02	−395.421 56	−783.588 13	−783.58 813			0.144 97
Nap-2-SH[d]	−395.921 60	−396.047 90	−784.217 42	−784.217 42			0.153 33
2	−563.272 48	−563.452 86	−2115.922 73	−2116.886 94	−2115.688 803	−2115.950 427	0.200 55
PhSSPh			−1259.863 22		−1259.678 176	−1259.876 768	0.194 68
CH_3SSCH_3			−876.289 803		−876.207 532 9	−876.300 824 4	0.083 87
1b	−563.879 90	−564.071 90	−2116.544 66	−2117.490 92			0.209 39
1a	−563.879 71						
6b	−1126.571 42		−4231.883 01		−4231.416 025	−4231.939 390	0.403 54
6c	−1126.5453						
5	−562.703 13		−2115.354 31				0.192 54
4	−562.673 09		−2115.325 61				0.192 07
3b	−834.202 60						
3a	−834.203 18						

[a] Single-point electronic energies calculated using the basis set indicated with geometries optimized at the B3LYP/LANL2DZ ECP level of theory (UB3LYP for open shell systems). ELANL2DZ uses the LANL2DZ ECP (Mo) and the 6-311++G(2d,2p) basis set (CHS). ECEP-121G uses the CEP-121G ECP basis on Mo and the 6-311++G(2d,2p) functions on C,H,S. [b] The electronic energy of hydrogen atom was set to −0.5 hartree for BDE calculations. [c] Naphthalene-2-thiyl radical. [d] 2-Mercaptonaphthalene. [e] Geometry optimized using B3LYP/LANL2DZ ECP for Mo and 6-31G* for CHS. [f] Single-point energy at B3LYP/LANL2DZ (Mo) and 6-311++G(2d,2p) (CHS) on geometry of footnote e. [g] B3LYP/LANL2DZ ECP frequencies used for thermal corrections.

Table 4. UB3LYP S−H Bond Dissociation Enthalpies (298 K), kcal/mol, from Semidirect, Equation 31 (D) and Isodesmic, Equation 32 (I) Calculations (B3LYP/LANL2DZ Geometries Employed)

	H_2S (expt 91.2)	**1**		PhSH (expt 79.1)[b]		Nap-2-SH (expt 77.9)[b]		CH_3SH (expt 87.3)[b]	
basis set	D	D	I	D	I	D	I	D	I
LANL2DZ	78.7	63.3	76.6	67.8	81.1	66.9	80.3	75.3	88.7
LANL2DZdp	88.0	70.6	74.7	76.6	80.6	75.5	79.6	84.3	88.4
ELANL2DZ[a]	90.4	72.5	73.2	78.5	79.3	77.4	78.1	86.9	87.7
ECEP-121G[a]	90.4	72.2	73.0	78.5	79.3	77.4	78.1	86.9	87.7

[a] See footnote a, Table 3. [b] Reference 34 and references therein.

Discussion

Benzyl Radical Selectivities in Hydrogen Atom Abstractions of Aryl, Alkyl, and Molybdenum Thiols and a Molybdenum Hydride. The rate constant for hydrogen atom abstraction by benzyl radical from **1** at 298 K (2.6×10^6 M^{-1} s^{-1}) is 20-fold faster than hydrogen abstraction from 2-mercaptonaphthalene and 100-fold faster than abstraction from octanethiol. The enhanced rates of hydrogen atom transfer from **1** to benzyl radical suggest a significant reduction in the S−H bond strength of **1**. Electronic structure calculations were carried out to estimate the SH bond strength, DH°, of **1** by direct dissociation (eq 31) and by the use of isodesmic calculations to calculate $\Delta H°_{298}$ for eq 32 followed by application of the bond strength of H_2S, 91.2 kcal/mol, as a reference (eq 32):

$$RSH \rightarrow RS^{\bullet} + H^{\bullet} \qquad (31)$$

$$RSH + HS^{\bullet} \rightarrow RS^{\bullet} + H_2S \qquad (32)$$

Calculated values of bond strengths by direct dissociation, e.g., eq 31, typically result in bond strengths lower than experiment that converge toward experimental values with improved basis set (Table 3). Bond strengths derived from isodesmic (and isogyric)[27] reactions (eq 32) tend to converge toward experimental values at a somewhat more modest basis set than required for accurate prediction by semidirect (eq 31) methods or by computing heats of atomization of molecules by CBS and related methods[28] not practicable for systems of the size of **1** and **2**. These trends are evident in Table 4. For H_2S, thiophenol, 2-mercaptonaphthalene, and CH_3SH, the errors in BDE average −0.6 kcal/mol (eq 25), and errors in the isodesmic BDEs average +0.3 kcal/mol at the highest level of theory (Table 4). At the UB3LYP/ELANL2DZ//LANL2DZ level of theory, the bond dissociation energies have converged to within 1 kcal/mol for all of the model thiol systems. From the pattern of convergence of the two computational approaches, the bond strength of **1** is predicted to be 73 kcal/mol. Inclusion of a larger, triple-ζ quality basis set at Mo (CEP-121G) yielded only slight change in the predicted bond strength.

Structural Assignment of Isomers of 1, 3, and 6. LANL2DZ ECP calculation of relative energies of the five isomers of **1** reveals the favored isomers to be those substituted on opposing sulfur bridges (**1a**,**b**):

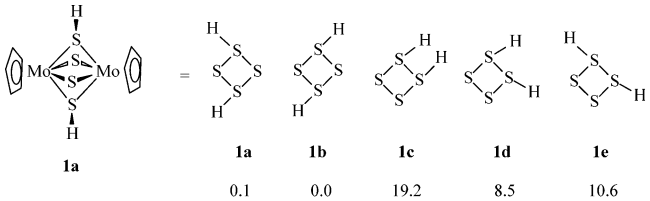

(27) Cramer, C. J. *Essentials of Computational Chemistry, Theories and Models*; John Wiley & Sons Ltd.: Chichester, West Sussex, U.K., 2003.

In agreement with M. Rakowski-Dubois and co-workers, who assigned the more stable of the isomers of **1** to the two trans isomers (**1a**,**b**),[8] DFT calculations predict **1b** and **1a** to be more stable than the three cis isomers, **1c**−**e**, by 10−20 kcal/mol. The electronic energies of **1a**,**b** and **3a**,**b** are too close to reliably assign **a** and **b** isomers.

Dimers **6** are also favored that have substituents on the sulfur bridge opposing the disulfide link. Thus, **6b**, with hydrogen atoms at remote bridge sulfur atoms in a transoid relationship to the disulfide bridge, is about 16 kcal/mol more stable than **6d**, which has a hydrogen atom attached to the sulfur bridge adjacent to the disulfide bond.

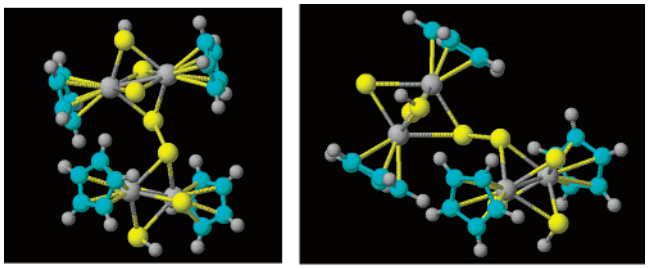

Isomer **6b**
HF=-1126.5714 hartree

Isomer **6d**
HF=-1126.5453 hartree

Thus, isomers of **1**, **3**, and **6** favor alkyl or hydrogen atoms disposed on nonadjacent bridge sulfur atoms. Because of the close proximity in energy found for the favored isomer pairs (**1a**,**b**; **3a**,**b**; and **6**), the assignments (**a**,**b**) for the isomers may be reversed in the discussions above. It is interesting to note that the electron density of the HOMO of **2** in Figure 4 is suggestive of favored bond formation at the sulfur opposed to the S−H group.

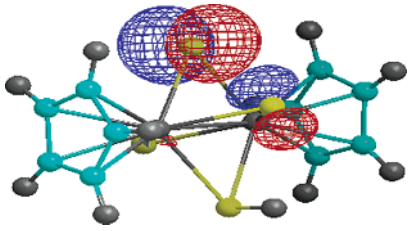

Figure 4. HOMO of radical **2** formed by hydrogen atom abstraction from **1**. Unpaired spin density is localized primarily on the μ-S bridge oppsite the S−H group.

Combination and Disproportionation Reactions of 2. The photolysis experiments of DBK and **1** revealed that benzyl radical undergoes cross-combination reactions with radical **2** to the near exclusion of cross-disproportionation (k_{comb}/k_{disp} > **3**/**5** > 20:1):

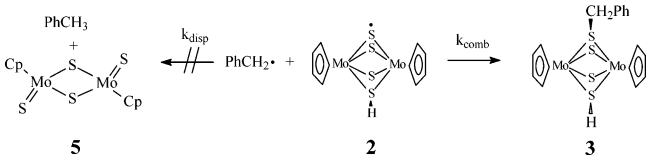

5 **2** **3**

Self-reaction of **2** in the absence of reactive radicals produces no detectable dimer(s) **6**, but only **5**:

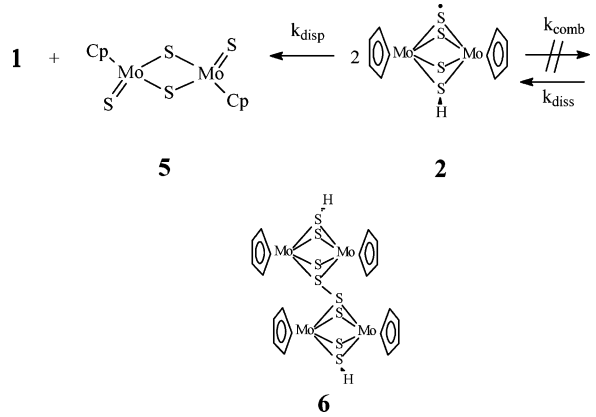

5 **2**

6

The above observations suggest that both self-combination and self-disproportionation of **2** are quite slow processes, whereas reaction of **2** with benzyl radical is a fast, diffusion-controlled process. The preference of **2** to form **5** rather than **6** may be related to steric congestion in forming the S−S bond of **6**. DFT calculations (B3LYP/ELANL2DZ//B3LYP/LANL2DZ) predict a 2.43 Å S−S bond for **6b**, longer than typical dialkyl disulfide bonds, 2.05−2.07 Å, and longer than a reported S−S bond length, 2.147 Å, of the related dicationic complex $[(MeCpMo(\mu\text{-}S))_2S_2CH_2]_2$ $(SO_3CF_3)_2$.[17] Thus, the modest basis set LANL2DZ ECP, lacking d-type functions on S, was inadequate for predicting the S−S bond length of **6b**. The geometry of **6b** was thus optimized with a hybrid basis set consisting of LANL2DZ ECP at Mo and the all-electron 6-31G* basis (CHS) giving an improved bond length of 2.08 Å for **6b**. Optimization of the geometry of $[(MeCpMo(\mu\text{-}S))_2S_2CH_2]_2$ $(SO_3CF_3)_2$ at the latter basis yielded an S−S bond length of 2.168 Å, in good agreement with the experimental data. Errors in calculated bond lengths are less than 0.03 Å, and errors in bond angles are less than 2°. (See the Supporting Information for a detailed comparison of bond lengths and bond angles for the dimer $[(MeCpMo(\mu\text{-}S))_2S_2CH_2]_2$.) Although the structural predictions are reliable, the error in bond strengths from direct dissociation calculations remains consistently low by about 10 kcal/mol. However, the magnitude of error in describing sulfur-centered radicals is consistent for arylthiyl and alkanethiyl radicals, allowing useful, if semiquantitative, estimates of bond strengths in isodesmic calculations. For example, the difference between S−S bond strengths in PhSSPh and CH_3SSCH_3 is predicted to be 17.5 kcal/mol (experiment 16 kcal/mol (Table 5)). The S−S bond strength of **6b** is thus estimated using isodesmic reactions, using thermochemical data from Table 5 with single-point electronic energies calculated at B3LYP/LANL2DZ ECP (Mo) and 6-311++G(2d,2p) (CHS) on the B3LYP/LANL2DZ ECP (Mo) and 6-31G* (CHS) geometries, together with thermal enthalpy corrections to 298 K:

$$DH°(\mathbf{6b}) = (PhSSPh(expt) - (PhSSPh(calcd) - \mathbf{6b}\ (calcd)) = 49.5 - (38.6 - 22.7) = 34\ kcal/mol$$

$$DH°(\mathbf{6b}) = CH_3SSCH_3(expt) - (CH_3SSCH_3\ (calc) - \mathbf{6b}\ (calc)) = 65.4 - (56.1 - 22.7) = 32\ kcal/mol$$

The exercise yields an estimate of 33 kcal/mol for the S−S bond of **6b**. This result, even allowing for substantial composite error (perhaps as much as 10 kcal/mol) in the calculations and in the experimental thermochemistry, predicts that **6b** should

(28) Henry, D. J.; Sullivan, M. B.; Radom, L. J. *J. Chem. Phys.* **2003**, *118* (1) 4849−4860.

Table 5. Thermochemical Values, kcal/mol, for Estimation of Isodesmic S−S Bond Strengths

species	$\Delta H°_{f,298}$	DH°, S–H	DH°, S–S (expt)	DH°, S–S (calcd)[g] direct (isodesmic)
PhSH	26.9[a]	79.1[e]		
CH_3SH	−5.5[b]	87.3[f]		
PhSSPh	58.3[c]		49.5	38.6(47)
CH_3SSCH_3	−5.8[d]		65.4	56.1(68)
6b				22.7(33)
PhS•	53.9			
CH_3S•	29.8			

[a] Scott, D. W.; McCullough, J. P.; Hubbard, W. N.; Messerly, J. F.; Hossenlopp, J. A.; Frow, F. R.; Waddington, G. *J. Am. Chem. Soc.* **1956**, *78*, 5463. [b] Good, W. D.; Lucina, J. L.; McCullough, J. P. *J. Phys. Chem.* **1961**, *65*, 2229. [c] Mackle, H.; Mayrick, R. G. *Trans. Faraday Soc.* **1962**, *50*, 238. [d] Hubbard, W. N.; Douslin, D. R.; McCullough, J. P.; Scott, D. W.; Todd, S. S.; Messerly, J. F.; Hossenlopp, J. A.; George, A.; Waddington, G. *J. Am. Chem. Soc.* **1958**, *80*, 3547. [e] Bordwell, F. G.; Zhang, X.-M.; Satish, A. V.; Cheng, J.-P. *J. Am. Chem. Soc.* **1994**, *116*, 6605. [f] *CRC Handbook of Chemistry and Physics*, 76th ed.; Lide, D. R., Ed.; CRC Press: Boca Raton, FL, 1995. [g] Single-point energies at B3LYP/LANL2DZ ECP (Mo) and 6-311++G(2d,2p) (CHS) calculated using the B3LYP/LANL2DZ ECP (Mo) and 6-31G* (CHS) geometry data and total thermal corrections of Table 3 to obtain direct dissocation values and isodesmic values in parentheses.

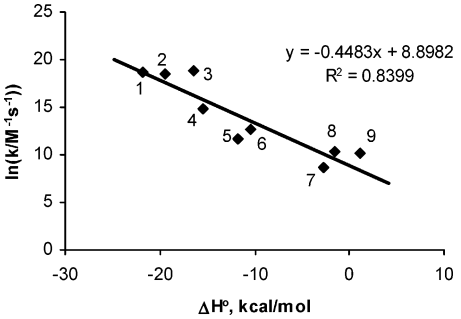

Figure 5. Plot of natural logarithm of abstraction rate constant, 298 K (carbon-centered radical, thiol) vs enthalpy of reaction: (1) *n*-Bu, PhSH; (2) *i*-Pr, PhSH; (3) *t*-Bu, PhSH; (4) benzyl, **1**; (5) benzyl, naphthyl-2-SH; (6) benzyl, PhSH; (7) PhCH(•)Ph, PhSH; (8) benzyl, *n*-octylSH; (9) PhC(•)OHCH$_3$, PhSH. Experimental values are taken from this work and from the following: Franz, J. A.; Bushaw, B. A.; Alnajjar, M. S. *J. Am. Chem. Soc.* **1989**, *111*, 268−275. Alnajjar, M. S.; Franz, J. A. *J. Am. Chem. Soc.* **1992**, *114*, 1052−1058. Kandanarachchi, P. H.; Autrey, T.; Franz, J. A. *J. Org. Chem.* **2002**, *67*, 7937−7945.

not decompose homolytically to regenerate **2** at an appreciable rate at ambient temperatures and should have been readily detectable. The S−S bond strength of **6b** is appreciably less than that of PhSSPh and may reflect significant strain built into the crowded $Cp_4Mo_4S_8H_2$ cluster. This finding may be related to the failure of radical **2** to combine to form **6**.

Evans−Bell−Polanyi Correlation of Hydrogen Atom Transfer Reactivity. The reactivity for hydrogen atom transfer to carbon-centered radicals from thiols in nonpolar solvents is broadly correlated with $\Delta H°$ for the S−H atom transfer reaction.[29] As depicted in Figure 5, rate constants for hydrogen atom transfer range from $\sim 10^8$ M^{-1} s^{-1} for reaction of primary radicals with thiophenol ($\Delta H° = -22$ kcal/mol) to 3×10^3 M^{-1} s^{-1} for reaction of a stabilized benzylic radical, PhCH(•)(OH)CH$_3$, with thiophenol ($\Delta H° = 2$ kcal/mol) to 6 M^{-1} s^{-1} for reaction of triphenylmethyl radical with thiophenol.[30] The value of $\ln(k_{abs}/M^{-1}\ s^{-1})$ for reaction of benzyl radical with **1** is plotted against the value of $\Delta H° = -15.5$ kcal/mol from the theoretically predicted value of 73 kcal/mol for the S−H bond of **1**, compared to $\Delta H° = -13 \pm 4$ kcal/mol predicted from the relationship of Figure 5.

A pattern of reactivity of the donating species shows an increase in rate constants by about an order of magnitude from 1-octanethiol to 2-mercaptonaphthalene to $[CpMo(\mu\text{-}S)(\mu\text{-}SH)]_2$. ($Cp^*Mo(CO)_3H$ is included in Table 1 to illustrate the reactivity of a directly Mo-bonded hydrogen atom compared to the reactivity of the MoS−H group. The reactivity increases by a factor of 6 on going from **1** to $Cp^*Mo(CO)_3H$, DH° = 69 kcal/mol.[31] Steric crowding about the molybdenum hydride and interaction of the bulky substituents about the α-carbon of the abstracting radical with the inaccessible Mo−H exert significant control over the rates of hydrogen atom donation for $Cp^*Mo(CO)_3H$.[13]) For $[CpMo(\mu\text{-}S)(\mu\text{-}SH)]_2$, **1**, the radially disposed S−H groups appear readily accessible to abstracting radicals, with substantial separation from the Cp groups. The radical **2**, while apparently disfavoring self-combination, readily undergoes cross-combination with transient, reactive radicals on the periphery of the S_4 ring. The dimethyl analogue of the molybdenum dithiol complex, $[CpMo(\mu\text{-}S)(\mu\text{-}SCH_3)]_2$, reveals a pseudo square planar array of sulfur atoms approximately the size of a cyclopentadienyl ring.[8] This suggests that the hydrosulfido ligands on $[CpMo(\mu\text{-}S)(\mu\text{-}SH)]_2$ would be fully exposed and unhindered by the distant Cp ligands. This assumption is confirmed by the observed reactivity order shown in Figure 5, on assignment of the calculated estimate of DH° = 73 kcal/mol for the S−H bond of **1**.

Conclusions

The first kinetics of reaction of a carbon-centered radical with the μ_2-S−H group in a Mo_2S_4 cluster are reported. New temperature-dependent rate data for abstraction of hydrogen atom from a μ_2-S−H group of the transition metal dithiol, **1**, have been measured, together with new absolute rate expressions for abstraction of arene- and alkane-thiol S−H hydrogen atoms by benzyl radical. The observed trend in reactivity is semiquantitatively correlated in a Polanyi relationship and found to be consistent with the 73 kcal/mol S−H bond strength predicted for **1** by DFT calculations. The reduced S−H bond strength of **1**, in comparison to organic thiols, suggests that the Mo(μ_2-S−H)Mo group will be more reactive in reverse-radical-disproportionation (RRD) pathways than conventional organic thiols and in reactions involved in the catalysis of hydrogenation/dehydrogenation pathways involving MoS catalyst substructure. Accordingly, Mo(μ_2-S−C)Mo bond strengths are lower than conventional thiols, enhancing homolytic S−C bond cleavage in HDS for nonpromoted catalysts. For promoted catalysts, addition of a third metal center, $CoMo_2(\mu_3\text{-}S{-}H)$ and $CoMo_2(\mu_3\text{-}S{-}C)$ may further dramatically lower S−H and S−C homolytic bond strengths.[4] Finally, radical **2** exhibits properties of favoring cross-termination with reactive alkyl radicals but does not undergo combination to the dimer and only undergoes disproportionation very slowly in the absence of reactive transient radicals, fitting the definition of a persistent free radical. The build-in of strain on formation of **6** results in a weakened S−S bond and may contribute to the strongly disfavored dimerization of **2**.

(29) Evans, M. G.; Polanyi, M. *Trans. Faraday Soc.* **1938**, *34*, 11.
(30) Colle, T. H.; Glaspie, P. S.; Lewis, E. S. *J. Org. Chem.* **1978**, *43*, 2722−2725.
(31) (a) Nolan, S. P.; Lopez de la Vega, R.; Hoff, C. D. *Organometallics* **1986**, *5*, 2529. (b) Reference 6a.

Electronic Structure Calculations. Geometry optimizations were carried out using the B3LYP[32] density functional with the LANL2DZ ECP basis set which includes the D95[33] basis set on first row elements and the Los Alamos ECP plus D95 basis set for second row and higher elements,[34] using the Gaussian 98[35] or NWChem 4.5[36] programs. Single-point calculations were carried out with the LANL2DZ geometries of the Mo species and organosulfur species using three basis sets, (1) the LANL2DZ ECP basis set augmented with diffuse and polarization functions, LANL2DZdp,[37] (2) a basis set (denoted ELANL2DZ) consisting of the LANL2DZ ECP basis set for Mo enhanced with the 6-311++G(2d,2p) basis set for H, C, and S, and (3) ECEP-121G, corresponding to the CEP-121G ECP[38] basis set for Mo and the 6-311++G(2d,2p)[39] basis set for C, H, and S. For examination of S−S bonding in structures **6**, geometries were optimized at B3LYP/LANL2DZ ECP (Mo) and 6-31G* (CHS) with single-point energies calculated at B3LYP/LANL2DZ ECP (Mo) and 6-311++G(2d,2p) (CHS). Analytical gradient calculations were employed to confirm ground states and to correct electronic energies to ambient temperature enthalpy values. Total enthalpy corrections to the electronic energy at 298 K were computed according to eq 30:[40]

$$H_{298}^{\circ} = {}^{3}/_{2}RT + nRT + R\sum_{k}(\Theta_{k,a}({}^{1}/_{2} + 1/(e^{\Theta_{k,b}/T} - 1))) + RT \quad (30)$$

$$\Theta_{k,x} = (c_1)hc/k_b\lambda_k$$

$n = 1$, linear: $x = a$, $c_1 = 0.9806$

$n = 3/2$, nonlinear: $x = b$, $c_1 = 0.9989$

Equation 30 includes a translational, a rotational, an internal (ZPE and vibrational), and a PV term. Each vibration, λ_k, was scaled by 0.9806 for the ZPE term ($x = a$) and by 0.9989 for the vibrational term ($x = b$).[41] Each vibration was examined to identify group rotations, and scaled internal rotations under 260 cm^{-1} were replaced by $^{1}/_{2}RT$. The electronic energy for the hydrogen atom was taken as −0.5 hartree. The present approach resembles the methodology of DiLabio et al.[42] with exception of the use of UB3LYP treatment of open shell systems. Electronic energies and total thermal corrections are presented in Table 3, and calculated bond dissociation energies are presented in Table 4. Cartesian coordinates for B3LYP/LANL2DZ geometries are available in the Supporting Information.

Experimental Section

Reagents. $[CpMo(\mu\text{-}S)(\mu\text{-}SH)]_2$ was synthesized using a literature procedure.[8] Phenylbenzyl ketone (PBK) and dibenzyl ketone (DBK) were purchased from Aldrich and recrystallized from methanol or purified by radial chromatography on silica gel using methylene chloride/hexane eluent. Benzene was purchased from Aldrich and triply fractionally distilled to reduce trace toluene to $\sim 10^{-7}$ M. 1-Octanethiol was purchased from Aldrich and distilled. Cyclohexane, *tert*-butylbenzene, and dichloromethane were purchased from Aldrich and used without further purification.

Rate Constants for Reaction of Benzyl Radical with $[CpMo(\mu\text{-}S)(\mu\text{-}SH)]_2$, 1-Octanethiol, and 2-Mercaptonaphthalene. Pyrex reaction tubes (5 mm) containing 200 μL of solution (0.02 M DBK or 0.02 M PBK, 10^{-4} M $[CpMo(\mu\text{-}S)(\mu\text{-}SH)]_2$ (or 0.01 M $CH_3(CH_2)_7SH$, or 2×10^{-3} M 2-mercaptonaphthalene), and 10^{-3} M *tert*-butylbenzene in benzene) were freeze−thaw degassed 3 times and flame sealed with an approximate headspace of 600 ± 50 μL. The tubes were placed inside a thermostated oven equipped with a quartz window and allowed to achieve temperature equilibrium for 1 min. The sample was photolyzed with a water-filtered 1-kW high-pressure xenon arc lamp for controlled periods of time (0.50−20.00 ± 0.005 s) using a Uniblitz model 225L0AOT522952 computer-controlled electronic shutter. Reagent concentrations were corrected for solvent vapor pressure and density.[43] Rate constants for hydrogen abstraction were calculated using eq 10c at 0.5−8.0 s photolysis times, using the measured product concentrations, the calculated average molybdenum-thiol donor concentration, and the benzyl self-radical termination rate, $2k_t$, calculated from the expression $\ln(2k_t/M^{-1}\ s^{-1}) = 27.23 - 2952.5/RT$. This expression was calculated using the von Smoluchowski equation, eq 33, using the Spernol−Wirtz modification of the Debye−Einstein equation, eq 34, where f in eq 34 is the SW microfriction factor.[44]

$$2k_t = (8\pi/1000)\sigma\rho D_{AB}N \quad (33)$$

$$D_{AB} = kT/6\pi r_A \eta f \quad (34)$$

Fischer and co-workers[45] have measured self-termination rate expressions for benzyl radical in cyclohexane, $\ln(2k_t/M^{-1}\ s^{-1}) = 26.2 - 2497.6/RT$, and in toluene, $\ln(2k_t/M^{-1}\ s^{-1}) = 27.05 - 2797.4/RT$. For self-termination of benzyl in hexane, we previously developed the expression $\ln(2k_t/M^{-1}\ s^{-1}) = 26.0 - 1803.6/RT$.[46] Parameters for estima-

(32) (a) Lee, C.; Yang, W.; Parr, R. G. *Phys. Rev. B* **1988**, *37*, 785. (b) Becke, A. D. *J. Chem. Phys.* **1993**, *98*, 5648.
(33) Dunning, T. H., Jr.; Hay, P. J. In *Modern Theoretical Chemistry*; Schaefer, H. F., III, Ed.; Plenum: New York, 1976; Vol. 3, p 1.
(34) (a) Hay, P. J.; Wadt, W. R. *J. Chem. Phys.* **1985**, *82*, 270. (b) Wadt, W. R.; Hay, P. J. *J. Chem. Phys.* **1985**, *82*, 284. (c) Hay, P. J.; Wadt, W. R. *J. Chem. Phys.* **1985**, *82*, 299.
(35) Frisch, M. J.; Trucks, G. W.; Schlegel, H. B.; Scuseria, G. E.; Robb, M. A.; Cheeseman, J. R.; Zakrzewski, V. G.; Montgomery, J. A., Jr.; Stratmann, R. E.; Burant, J. C.; Dapprich, S.; Millam, J. M.; Daniels, A. D.; Kudin, K. N.; Strain, M. C.; Farkas, O.; Tomasi, J.; Barone, V.; Cossi, M.; Cammi, R.; Mennucci, B.; Pomelli, C.; Adamo, C.; Clifford, S.; Ochterski, J.; Petersson, G. A.; Ayala, P. Y.; Cui, Q.; Morokuma, K.; Malick, D. K.; Rabuck, A. D.; Raghavachari, K.; Foresman, J. B.; Cioslowski, J.; Ortiz, J. V.; Stefanov, B. B.; Liu, G.; Liashenko, A.; Piskorz, P.; Komaromi, I.; Gomperts, R.; Martin, R. L.; Fox, D. J.; Keith, T.; Al-Laham, M. A.; Peng, C. Y.; Nanayakkara, A.; Gonzalez, C.; Challacombe, M.; Gill, P. M. W.; Johnson, B. G.; Chen, W.; Wong, M. W.; Andres, J. L.; Head-Gordon, M.; Replogle, E. S.; Pople, J. A. *Gaussian 98*, revision A.11; Gaussian, Inc.: Pittsburgh, PA, 2001.
(36) Straatsma, T. P.; Apra, E.; Windus, T. L.; Dupuis, M.; Bylaska, E. J.; de Jong, W.; Hirata, S.; Smith, D. M. A.; Hackler, M. T.; Pollack, L.; Harrison, R. J.; Nieplocha, J.; Tipparaju, V.; Krishnan, M.; Brown, E.; Cisneros, G.; Fann, G. I.; Fruchtl, H.; Garza, J.; Hirao, K.; Kendall, R.; Nichols, J. A.; Tsemekhman, K.; Valiev, M.; Wolinski, K.; Anchell, J.; Bernholdt, D.; Borowski, P.; Clark, T.; Clerc, D.; Dachsel, H.; Deegan, M.; Dyall, K.; Elwood, D.; Glendening, E.; Gutowski, M.; Hess, A.; Jaffe, J.; Johnson, B.; Ju, J.; Kobayashi, R.; Kutteh, R.; Lin, Z.; Littlefield, R.; Long, X.; Meng, B.; Nakajima, T.; Niu, S.; Rosing, M.; Sandrone, G.; Stave, M.; Taylor, H.; Thomas, G.; van Lenthe, J.; Wong, A.; Zhang, Z. *NWChem, A Computational Chemistry Package for Parallel Computers*, version 4.5; Pacific Northwest National Laboratory: Richland, WA 99352-0999, U.S.A., High Performance Computational Chemistry Group, Pacific Northwest National Laboratory, Richland, WA 99352, U.S.A., 2003.
(37) Check, C. E.; Faust, T. O.; Bailey, J. M.; Wright, B. J.; Gilbert, T. M.; Sunderlin, L. S. *J. Phys. Chem. A* **2001**, *105*, 8111.
(38) (a) Stevens, W.; Basch, H.; Krauss, *J. Chem. Phys.* **1984**, *81*, 6026. (b) Stevens, W. J.; Krauss, M.; Basch, H.; Jasien, P. G. *Can. J. Chem.* **1992**, *70*, 612. (c) Cundari, T. R.; Stevens, W. J. *J. Chem. Phys.* **1993**, *98*, 5555.
(39) (a) Krishnan, R.; Binkley, J. S.; Seeger, R.; Pople, J. A. *J. Chem. Phys.* **1980**, *72*, 650. (b) Blaudeau, J.-P.; McGrath, M. P.; Curtiss, L. A.; Radom, L. *J. Chem. Phys.* **1997**, *107*, 5016. (c) Clark, T.; Chandrasekhar, J.; Schleyer, P.v. R. *J. Comput. Chem.* **1983**, *4*, 294.
(40) McQuarrie, D. A. *Statistical Mechanics*; Harper and Row: New York, 1976.
(41) Scott, A. P.; Radom, L. *J. Phys. Chem.* **1996**, *100*, 16502.
(42) DiLabio, G. A.; Pratt, D. A.; LoFaro, A. D.; Wright, J. S. *J. Phys. Chem. A* **1999**, *103*, 1653−1661.
(43) (a) Reid, R. C.; Prausnitz, J. M.; Sherwood, T. K. *The Properties of Liquids and Gases*; McGraw-Hill: New York, 1977. (b) Weast, R. C.; Astle, M. J. *Handbook of Chemistry and Physics*; CRC Press: Boca Raton, FL, 1982−83.
(44) Fischer, H.; Paul, H. *Acc. Chem. Res.* **1987**, *20*, 200.
(45) (a) Lehni, M.; Schuh, H.; Fischer, H. *Int. J. Chem. Kinet.* **1979**, *11*, 705. (b) Claridge, R. F. C.; Fischer, H. *J. Phys. Chem.* **1983**, *87*, 1960. (c) Huggenberger, C.; Fischer, H. *Helv. Chim. Acta* **1981**, *64*, 338.

tion of the rate expression for self-termination of benzyl radical in benzene employed in these kinetics, $\ln(2k_t/M^{-1}\,s^{-1}) = 27.23-2952.5/RT$, are listed.[47] The maximum error in estimation of self-termination rate constants by this method is estimated to be less than ca. 25%.[44]

Photolysis of 1,3-Dibenzyl Ketone (DBK) and 1 in Benzene-d_6 for Product Analysis. A solution of **1** (0.005 M) and DBK (0.06 M) in degassed benzene-d_6 was photolyzed at room temperature with the diffused, water-filtered output of a 1-kW high-pressure Xe lamp for times varying from 0 to 3000 s. The photolysis solution was analyzed by ^{1}H NMR to obtain the spectra of Figure 3. Products phenylacetaldehyde, toluene, **3a**,**b**, and **8** were observed.

Photolysis of DBK and 1 in Benzene-d_6 with Prompt ^{1}H NMR Analysis. In the experiment above, the transient product **4** was not observed, possibly due to its decay during extended data acquisition times. Thus, a freeze−thaw degassed and sealed solution of DBK (0.05 M) and **1** (0.005 M) in benzene-d_6 in a Pyrex NMR tube was photolyzed with the unfiltered light of a 1-kW high-pressure Xe lamp. 50% conversion of **1** was obtained within several minutes, followed by prompt (within 5 min) analysis of the product mixture. At approximately 50% conversion of **1**, the observed products were toluene, phenylacetaldehyde, and **3a** and **3b**, the latter identified by the characteristic pairs of Cp, benzylic CH_2, and sulfhydryl groups (see Table 2). The Cp resonance assigned to **4** was present at low concentration, with a ratio **4**/(**3a** + **3b**) of 0.04.

Fast Atom Bombardment Mass Spectrometric Analysis. The above photolysis experiment in benzene-d_6 was repeated but terminated at ca. 50% conversion of **1**. The major products were **3a**, **3b**, and minor products were **8a**, **8b**. Solvent was removed in a vacuum, and the product mixture was analyzed by fast atom bombardment/electrospray ionization mass spectrometry (FAB/ESI). Multiple ion peaks corresponding to matrix-induced peaks $(CpMo)_2S_3$ (417.6), $(CpMo)_2S_4$ (449), and $(CpMo)_3S_4$ (613) were observed together with major peak groups corresponding to $(CpMo)_2S_4(H)(CH_2Ph)$ (**3**) (541) and $(CpMo)_2S_4(CH_2Ph)_2$ (**8**) (633).

Photolysis of Bu_tOOBu_t in Benzene-d_6. Observation and Decay of Transient 5. A solution of **1** (0.002 M) and Bu_tOOBu_t (0.17 M) in benzene-d_6 in a freeze−thaw degassed and sealed Pyrex NMR tube was photolyzed with a 1-kW unfiltered high-pressure xenon lamp. After 10 min of photolysis at room temperature, a single Cp peak at 5.78 ppm, assigned to **5**, was present at 2.7×10^{-4} M at 5 min of elapsed time following the end of photolysis. At 15, 25, 35, 55, 75, and 95 min, the concentration of **5** was found to be 2.64, 2.62, 2.58, 2.09, 1.86, and 1.63×10^{-4} M, corresponding to a half-life of 120 min, due to precipitation of highly insoluble **5**. No new sulfhydryl peaks were observed corresponding to **6** (e.g., in the region −1 to −3 ppm).

Exchange Reaction of 1 with $PhCH_2SH$ to Form 3 and 8. Similar to a procedure employed by Rakowski-DuBois and co-workers,[8] a freeze−thaw degassed solution of **1** (12 mg) and benzylthiol (3.5 uL) in $CDCl_3$ (1 mL) was heated at 65 °C for 18 h under 2 atm of H_2 in a sealed thick-walled NMR tube. ^{1}H NMR revealed complete conversion of **1** to **3a** (5.6%), **3b** (9.4%), **8a** (25%), and **8b** (60%). NMR data are presented in Table 2. (The identical reaction carried out in benzene-d_6 at room temperature for 8 days gave no exchange. When heated at 80°C for 5 h in benzene-d_6, **1** was converted to **3** in ca. 5% yield.)

Fast Atom Bombardment Mass Spectrometric Analysis. The above exchange experiment in $CDCl_3$ was repeated but with heating at 50 °C for 15 h and terminated at ca. 50% conversion of **1**. The major products were **3a**, **3b**, and minor products were **8a**, **8b**. Solvent was removed in a vacuum, and the product mixture was analyzed by fast atom bombardment/secondary ion mass spectrometry (FAB/LSIMS). Multiple ion peaks corresponding to matrix-induced peaks $(CpMo)_2S_3$ (417.6), $(CpMo)_2S_4$ (449.6), and $(CpMo)_3S_4$ (610.5) were observed together with major peak groups corresponding to $(CpMo)_2S_4(H)(CH_2Ph)$ (**3**) (540.6) and $(CpMo)_2S_4(CH_2Ph)_2$ (**8**) (632.5).

Attempted Chromatographic Fractionation of Exchange Products of $PhCH_2SH$ and 1 in $CHCl_3$. In a 200-mL vacuum flask, 420 mg of **1** (0.93 mmol), and 210 μL of benzylmercaptan (1.8 mmol) were dissolved in 100 mL of $CHCl_3$ and heated at 65 °C for 23 h. The reaction was evacuated to dryness and transferred in CH_2Cl_2 to an alumina column in a nitrogen glovebox. Three 30-mL fractions were collected with CH_2Cl_2 as eluent and taken to dryness, redissolved in $CDCl_3$ and benzene-d_6, and analyzed by ^{1}H and ^{13}C NMR. Fraction 1 contained 12% **1**, 7% **3a**, 12% **3b**, 1% **8a**, 68% **8b**. Fraction 2 contained 39% **1**, 11% **3a**, 18% **3b**, 27% **8a**, 6% **8b**. Fraction 3 contained 27% **1**, 3% **3a**, 5% **3b**, 64% **8a**, 1% **8b**. Careful spectroscopic (^{13}C and ^{1}H NMR) analysis of the fractions in $CDCl_3$ and benzene-d_6 allowed complete ^{1}H and ^{13}C spectral assignment of all isomers (Table 2). Note that the absolute **a**,**b** structural assignments of isomers of **3** and the **a**,**b** assignments of **8** are not established.

Oxidation of 1 to 5 in $CDCl_3$ and Benzene-d_6. A sample of **1** (15 mg) and *azo*-benzene (15 μL) in 1 mL of oxygen-free $CDCl_3$ was sealed in an NMR tube and then examined by ^{1}H NMR spectroscopy as a function of time over a period of 12 h. **1** (Cp in $CDCl_3$ at 6.38 ppm) was cleanly oxidized within 1 h to give 1,2-diphenylhydrazine and a single new Cp peak at 6.34 ppm, **5**. Over a period of 12 h, the peak assigned to **5** decreased in intensity to about 20% of peak value and less than ca. 1% by 20 h, accompanied by the deposition of solid material (reflecting very low solubility of **5**). The sample was opened on a vacuum line, charge with H_2 (1 atm) and resealed. Warming at 80 °C for 10 min led to restoration of **1** along with complete conversion of the remaining *azo*-benzene to 1,2-diphenylhydrazine. A second sample of **1**, 15 mg, and *azo*-benzene in 1 mL of benzene-d_6 was sealed in an NMR tube. **1** (Cp at 5.89 ppm in benzene-d_6) was cleanly and quantitatively converted to a single product with a Cp peak in the ^{1}H NMR spectrum at 5.78 ppm, **5**. The Cp resonance of **5** decayed to about 20% of its initial intensity over a period of about 10 h.

Acknowledgment. This work supported by the Office of Science, Office of Basic Energy Sciences, of the U.S. Department of Energy under Contract DE-ACO6-76RLO 1830. The authors thank Dr. Robert Barkley of the Central Analytical Laboratory, University of Colorado, Boulder, CO, for performing FAB analysis of reaction products of **1**.

Supporting Information Available: Tables of kinetic data, computational summaries from electronic structure calculations, and supporting spectral data. This material is available free of charge via the Internet at http://pubs.acs.org.

JA049321R

(46) Franz, J. A.; Suleman, N. K.; Alnajjar, M. S. *J. Org. Chem.* **1986**, *51*, 19.

(47) Diffusion coefficients D_{AB}, eq 7, were calculated for estimation of the self-termination rate of benzyl radical in benzene using the following data. For the radical model, toluene: mp 178 K, bp 383.8 K, MW 92.14, $\rho = 6.02 \times 10^{-8}$ cm (average of van der Waals (Edward, J. T. *J. Chem. Educ.* **1970**, *47* (4), 261), LeBas (Ghai, R. L.; Dullien, F. A. L. *J. Phys. Chem.* **1974**, *78*, 2283), and other (Spernol−Wirtz Spernol, A.; Wirtz, K. Z. *Naturforsch.* **1953**, *8a*, 522) diameters, $\sigma = {}^1/_4$, density of toluene, $d(T, K) = 1.1787-1.048 \times 10^{-3}$ (T, K). For the solvent benzene, mp 278.7, bp 353.3, MW 78.1, Andrade viscosity, $\ln(\eta, cP) = -4.117 + 2.0973 \times 10^3/RT$, $d(T, K) = 1.192-1.059 \times 10^{-3}(T, K)$. The microfriction factor ×a6 of Spernol and Wirtz is given by $\times a6 = (0.16 + 0.4r_A/r_B)(0.9 + 0.4T_A{}^r - 0.25T_B{}^r)$, and reduced temperatures are given by $T_X{}^r = (T - T_X{}^f)/(T_X{}^b - T_X{}^f)$, where $T_X{}^f$ and $T_X{}^b$ are freezing and boiling points of species X = benzyl (A) or benzene (B). The radii in the microfriction factor term are given by $r_X = (3V_X(\chi)/4\pi N)^{1/3}$, where $\chi = 0.74$, the volume fraction for cubic closest packed spheres, and V_X are density-based molecular volumes, and N is Avogadro's number. The resulting Smoluchowski expression for self-termination of the benzyl radical in benzene is $\ln(2k_t/M^{-1}\,s^{-1}) = 27.23-2952.47/RT$. A similar treatment for benzyl self-termination in toluene is in near-perfect agreement with experimental values (ref 42).